

1 Three-dimensional regional bi-ventricular
2 shape remodeling is associated with
3 exercise capacity in endurance athletes.
4

5 **Bernardino G^{1,2*}; Sanz de la Garza M^{3,4*}; Domenech-Ximenes B^{3,5}; Prat- González**
6 **S^{3,4}; Perea RJ⁶; Blanco I^{7,8}; Burgos F^{7,8}; Sepulveda-Martinez A^{9,10,11}; Rodriguez-**
7 **Lopez M^{9,10,12}; Crispi F^{9,10}; Butakoff C¹³; González Ballester MA^{1,14}; De Craene M²;**
8 **Sitges M^{3,4}; Bijmens B^{1,14}**

- 9 1. BCN Medtech, DTIC Universitat Pompeu Fabra, Barcelona, Spain
- 10 2. Medisys, Philips, Paris, France
- 11 3. Cardiovascular Institute, Hospital Clínic, IDIBAPS, Barcelona, Spain
- 12 4. CIBERCV, Barcelona, Spain
- 13 5. Radiology Department, Hospital Universitari Dr. Josep Trueta, Girona, Spain.
- 14 6. Radiology Department, IDIBAPS, Hospital Clínic, Barcelona, Spain
- 15 7. ICR, IDIBAPS, University of Barcelona, Barcelona, Spain
- 16 8. Biomedical Research Networking Center on Respiratory Diseases, Madrid; Spain.
- 17 9. BCNatal, ICGON, IDIBAPS, Universitat de Barcelona, Barcelona, Spain
- 18 10. CIBER-ER, Barcelona, Spain.
- 19 11. Fetal Medicine Unit, Department of Obstetrics and Gynecology Hospital Clínico de la
20 Universidad de Chile. Santiago de Chile, Chile.
- 21 12. Pontificia Universidad Javeriana Cali, Colombia
- 22 13. BSC, Barcelona, Spain
- 23 14. ICREA, Barcelona, Spain

- 24 • * Both authors contributed equally.
- 25 • **Corresponding author:** gabriel.bernardino@upf.edu
- 26

27 Abstract

28 **Aims:** Endurance athletes develop cardiac remodeling to cope with increased cardiac output
29 during exercise. This remodeling is both anatomical and functional and shows large
30 interindividual variability. In this study, we quantify local geometric ventricular remodeling
31 related to long-standing endurance training and assess its relationship with cardiovascular
32 performance during exercise.

33 **Methods:** We extracted 3D models of the biventricular shape from end-diastolic cine
34 Magnetic Resonance images acquired from a cohort of 89 triathlon athletes and 77 healthy
35 sedentary subjects. Additionally, the athletes underwent Cardio-Pulmonary Exercise Testing,
36 together with an echocardiographic study at baseline and few minutes after maximal
37 exercise. We used Statistical Shape Analysis to identify regional bi-ventricular shape
38 differences between athletes and non-athletes.

39 **Results:** The ventricular shape was significantly different between athletes and controls
40 ($p < 1e-6$). The observed regional remodeling in the right heart was mainly a shift of the right
41 ventricle (RV) volume distribution towards the right ventricular infundibulum, increasing the
42 overall right ventricular volume. In the left heart, there was an increment of left ventricular
43 mass and a dilation of the left ventricle. Within athletes, the amount of such remodeling was
44 independently associated to higher peak oxygen pulse ($p < 0.001$) and weakly with greater RV
45 Global Longitudinal Strain reserve ($p = 0.03$).

46 **Conclusions:** We were able to identify specific bi-ventricular regional remodeling induced by
47 long-lasting endurance training. The amount of remodeling was associated with better
48 cardiopulmonary performance during an exercise test.

49

50 **Keywords:** exercise physiology, athlete's heart, cardiac remodeling, statistical shape analysis

51 Abbreviation List

- 52 • AUROC: Area under receiver operator characteristic
- 53 • BSA: body surface area
- 54 • CO: cardiac output
- 55 • CPET: cardiopulmonary exercise testing
- 56 • HR: heart rate
- 57 • LH: left heart
- 58 • LOO-CV: leave one out cross validation
- 59 • LV: left ventricle
- 60 • LVGLS: left ventricular global longitudinal strain

- 61 • LVOT: left ventricular outflow tract
- 62 • MRI: magnetic resonance imaging
- 63 • PCA: principal component analysis
- 64 • PER: pulmonary extraction ratio
- 65 • PLS: partial least squares
- 66 • RA: right atria
- 67 • RH: right heart
- 68 • RV: right ventricle
- 69 • RV-FW: right ventricular free wall
- 70 • RVGLS: right ventricle global longitudinal strain
- 71 • RVOT: right ventricle outflow tract
- 72 • SA: short axis
- 73 • SSA: statistical shape analysis
- 74 • STD: standard deviation
- 75 • VO₂: oxygen uptake

76 Background

77 As reported in the literature, extensive periods of physical exercise result in chronic exposure
78 to volume and pressure overload, inducing cardiac remodeling (La Gerche et al. 2013; Schmier
79 and Borjesson 2014). This cardiac remodeling includes a set of morphological and functional
80 changes to obtain a better cardiovascular response to exercise. Known examples of such
81 remodeling are left ventricle (LV) hypertrophy and dilatation, dilated right ventricle (RV) and
82 atria (RA), decreased resting heart rate (HR) and a slight decrease in myocardial deformation
83 at rest. These changes vary importantly among individuals, but remodeling is consistently
84 more present in the Right Heart (RH) (Rhodes et al. 1990; La Gerche et al. 2012; D'Andrea et
85 al. 2015), which is exposed to a bigger relative pressure increase during exercise in comparison
86 to baseline than the left heart (LH). Exercise-induced remodeling is known to be influenced by
87 lifestyle parameters such as sport discipline, training load and individual-specific parameters
88 such as age, gender, ethnicity (Sanz-de la Garza et al. 2017; Sitges et al. 2017). However, the
89 details and spectrum of physiological adaptation to sport is not yet completely understood.

90 Geometric assessment of cardiac structures in the clinical community is still predominantly
91 focusing on sparse length/volumes measurements rather than 3D shape patterns. These
92 measurements are insufficient to analyze regional differences, and especially cannot account
93 for the RV shape complexity and variability. Statistical Shape Analysis (SSA) denotes a set of
94 techniques that compute a reference shape for a population and subsequently describe each
95 individual shape with the transformation from the template to this individual (Dryden and
96 Mardia 1998). These techniques have been applied to find regional morphology and
97 deformation differences between two different populations (De Craene et al. 2012; Zhang et
98 al. 2014; Varela et al. 2017; Varano et al. 2018).

99 This paper uses SSA methods to find regional differences between bi-ventricular shapes, as
100 retrieved from magnetic resonance imaging (MRI), of endurance athletes and non-athletes
101 and relate these to exercise response and classical imaging parameters. Given that the RH
102 plays a crucial role during exercise, and that its complex shape is difficult to assess using
103 traditional clinical image-based measurements, the proposed approach is particularly suited
104 to study exercise-induced shape alteration in the RH.

105

106 Methods

107 Population

108 A cohort of healthy 89 triathlon athletes and 77 controls was recruited at Hospital Clínic,
109 Barcelona, according to an internal research protocol validated by the internal ethical
110 committee, and written informed consent was obtained for each of the participants. The
111 triathlete inclusion criteria implied that they exercised at least 10 hours weekly for at least 5
112 years. They were evaluated via a physical activity questionnaire (Ainsworth et al. 2011).
113 Controls were randomly selected from the birth registry between years 1975 and 1995 in a
114 tertiary university hospital in Barcelona. All individuals included in this study were
115 asymptomatic with no previous known cardiovascular illnesses and no cardiac disease
116 detected on echocardiography.

117 Echocardiographic measurements

118 Echocardiographic images for athletes were acquired with a commercially available ultrasound
119 system (Vivid Q; GE Medical; Milwaukee, USA) with a 2.5 MHz (M5S) and an active matrix 4-
120 dimensional volume phased array transducer in the case of the controls. Images were acquired
121 from the parasternal (long- and short-axis) and apical (RV-focused 4-, 4-, 3- and 2-chamber)
122 views. Three consecutive cardiac cycles for each acquisition were digitally stored in a cine loop
123 format for off-line analysis with commercially available software (EchoPac GE, Vingmed).
124 Cardiac chamber dimensions were measured according to the standards of the European
125 Society of Echocardiography and indexed for body surface area according to the DuBois
126 formula (Du Bois and Du Bois 1916). RV end-diastolic area and end-systolic area were estimated
127 by tracing the endocardium from a RV-focused apical 4-chamber view. LV volumes and LV
128 ejection fraction were derived using the biplane Simpson method. Myocardial deformation of
129 both ventricles was evaluated by 2D-STE (2Dstrain, Echo Pac, version 202.41.0, General Electric
130 Healthcare, Milwaukee, WI, USA). Global RV peak systolic strain (RVGLS) was measured as an
131 average of all six RV segments (3 RV-FW and 3 inter-ventricular septum). Left ventricle global
132 longitudinal strain (LVGLS) was calculated as an average of LV systolic strain in 2-, 3- and 4-
133 chamber apical views (Lang et al. 2015).

134 Exercise Test

135 All individuals performed a standard incremental cardiopulmonary exercise testing in an
136 up-right position on an electrically braked cycle ergometer (range 6-999 watts) using an
137 Ergoselected 100 (Ergoline, Bitz, Germany). Over the course, of this test, they performed an
138 increasingly demanding exercise until exhaustion, while their gas exchange parameters and
139 HR were being monitored using a breath-by-breath and a 12 lead ECG. From this, the peak
140 and basal oxygen uptake, as well as the HR were measured using the ExpAir software
141 (Medisoft, Sorinnes, Belgium). All measurements were performed according to international
142 guidelines (Ross et al. 2003; Albert et al. 2008).

143 Athletes were subjected to a post-exercise echocardiographic exam. Immediately after the
144 end of the exercise test, they were moved to a bed next to the ergometer and were scanned
145 to assess function and geometry changes occurring during exercise.

146 MRI study

147 Cardiac MRI studies were performed using a 3T (72 athletes and 77 controls) or 1.5T (17
148 athletes) scanner (Magnetom Trio Tim and Magnetom Aera respectively, *Siemens Medical*
149 *Solutions, Erlangen, Germany*) in all subjects involved in this protocol. Images were acquired
150 during apnea. A cine sequence in short axis (SA) view was acquired with 8mm slice thickness,
151 an interslice gap ranging from 0 to 2.4mm, and a pixel size ranging between 0.8 to 1.5 mm.

152 For each individual in our population, we generated a 3D surface by fitting a whole-heart
153 deformable template, for all time instances, to the SA MRI, using the algorithm described
154 and validated in (Ecabert et al. 2006; Peters et al. 2010). From this, we extracted the LV end-
155 diastolic (ED) frame and selected the LV epicardial and endocardial surfaces as well as the RV
156 endocardium. All contour points were in one-to-one correspondence due to the model-
157 based segmentation.

158 An expert visually checked all automatic segmentations in the SA, and 2 individuals were
159 discarded for inadequate tracing of the ventricular contour. In the supplementary material S1
160 we show randomly selected examples of the segmentation contours.

161

162 Statistical Shape Analysis

163 We represented the surfaces/shapes by a Point Distribution Model (PDM) (Cootes et al.
164 1995), and we used Partial Procrustes Analysis to rigidly align each individual to a common
165 position, thus removing positioning-related variability.

166 We used Principal Component Analysis (PCA), and Partial Least Squares (PLS) to build a
167 dimensionality reduction that encoded most of the shape variability that correlated with the
168 athlete label. First, we used PCA to obtain a dimensionality reduction that kept 95% of the
169 shape variability, serving as a denoising step. Then, we used PLS to further reduce the shape
170 space to 4 modes that maximized covariance with the athlete label. Finally, we used Logistic
171 Regression (LR) to find an optimal separation between athletes and controls in that reduced
172 space, adjusting by BSA, age and gender as covariates. This LR corresponded to a certain
173 shape pattern, the *athletic remodeling*, that subsequently could be quantified for each
174 individual and expressed as a *remodeling score*.

175 To verify the model's invariance to age and gender, we used the same SSA method as
176 described above to obtain the athletic remodeling shape pattern, after gender-stratifying the
177 population, as well as with an age-equalized subpopulation. We computed the Pearson's
178 correlation coefficient between remodeling scores obtained with the restricted datasets and
179 the remodeling scores derived from the full dataset.

180 Statistical methods

181 We tested the difference of scalar variables using the Mann-Whitney U-test, and the Chi-
182 Square test for categorical variables. We used Multivariate Regression (MVR) to assess the
183 relationship between the athletic remodeling score and the scalar measurements,
184 independently of the confounding variables (BSA, gender and age) that are introduced as
185 covariates in the model. To assess the results of the MVR, we report the p-value using the
186 Fisher F-test, comparing with a model with only the confounding variables as predictors, and
187 the standardized regression coefficient associated with the remodeling score and the R^2
188 determination coefficient of the model as effect size.

189 The performance of a logistic model was evaluated using the Area Under Curve (AUC) of the
190 Receiver Operator Characteristic (ROC). We evaluated the models using leave one out cross
191 validation (LOOCV) to split the data in a derivation and validation cohorts without loss of
192 sample size. We compared the SSA model with a simple LR using the confounding variables
193 via a DeLong test (DeLong et al. 1988).

194 We implemented the analysis in Python 2.7.14 (Enthought Inc, Austin USA), with the
195 following packages: numpy (v1.13.0), scikit-learn(v0.18.1) and scipy(v0.19.0) and RStudio
196 1.1.423 (RStudio Inc, Boston MA) with package pROC(Robin et al. 2011). We set a threshold
197 of 0.05 to determine statistical significance.

198

199 Results

200 Population characteristics

201 The population demographics and functional echocardiographic-based parameters are
202 reported in Table 1. Athletes had a lower deformation, BSA and resting HR, which is consistent
203 with chronic exercise, and were 2 years older than controls. Their CO indexed by BSA is
204 maintained. Table 2 shows the comparison geometric MRI-based measurements between
205 athletes and controls. We found an overall increase of the ventricular size. Table S2.1 of the
206 supplementary material shows the difference between resting state and after maximal
207 exercise in athletes.

208 Athletic shape remodeling

209 We built a model that captures the differences in 3D shape between athletes and non-athletes
210 using our SSA technique described in the methodology. The model output is a shape pattern
211 that best discriminates between athletes and controls and is therefore the remodeling
212 acquired due to the practice of sport. To visualize that remodeling, in Figure 2 we show the
213 mean shape computed from the controls only, as well as the shape obtained by adding the
214 remodeling with 3 STD of the found athletic shape pattern, thus representing the shape of an
215 extreme athlete. Supplementary material S3 shows a continuous animation of this
216 remodeling. A qualitative assessment of the figure shows that shape remodeling is
217 concentrated in the RV: the outflow and RV apex of the extreme athlete are considerably
218 dilated and more spherical than the mean control. Finally, for each athlete, we quantified how
219 much of this athletic remodeling was present in their individual cardiac shape, to study the
220 relation to acute exercise response. We normalized such score to have 0 mean and 1 STD in
221 the controls.

222 Exercise response

223 Using MVR, we investigated in the athletes how different degrees of athletic shape
224 remodeling corresponded to cardiovascular performance in the stress test. *Table 3* shows
225 the standardized regression coefficients of the remodeling score with p-values. All models
226 used age, BSA and gender as covariates.

227 We found a negative association of athletic shape remodeling to both resting and maximal
228 HR ($p=0.03$, $R^2=0.08$; $p=0.08$, $R^2=0.19$ respectively). Resting VO_2 was not associated to
229 athletic remodeling, but peak VO_2 and peak O_2 pulse were ($p<0.01$, $R^2=0.49$; $p<0.001$,
230 $R^2=0.51$). There was an association between athletic remodeling and greater RVGLS reserve
231 ($p=0.03$, $R^2=0.24$). Neither resting nor post-exercise LVGLS were associated to shape
232 remodeling. While the athletic remodeling score was associated with larger cavities at rest,
233 we found no association with acute RV/LV dilation during the maximal stress test.

234 Validation

235 We compared the AUC of the shape's model (AUC = 0.91) and that of a LR that only takes
236 confounding variables into account (AUC = 0.71). The improvement due to the inclusion of
237 shape was statistically significant according to the DeLong test ($p<1e-6$). The ROC of both
238 models can be found in supplementary material S4. In supplementary material S5, we
239 compared our athletic remodeling score with the classical indices used to assess athletic

240 morphological remodeling (LV mass, LVEDV, RVEDV). Our score was very correlated to these
241 indices and had a slightly better performance at discriminating athletes and controls.

242 The gender stratified models presented a very strong correlation with the pooled model ($\rho =$
243 0.92 for the females-only model, and $\rho = 0.93$ for the males-only model). While we
244 observed no gender differences in the most discriminative shape pattern, men presented a
245 higher quantity of remodeling than women. The full experiments for the gender stratified
246 models can be found in the supplementary material S7. The age equalized model presented
247 an almost perfect with the pooled model ($\rho = 0.98$). The full results regarding age can be
248 found in the supplementary materials S7.

249

250 Discussion

251 Complementary to the well-known differences in size and mass, we found strongly
252 significant statistical differences in resting ventricular regional shape between athletes and
253 controls. Within athletes, those differences are positively associated with better
254 performance in an exercise test, as measured by VO_2 uptake. There was a small, yet
255 significant ($p=0.03$), positive relation with RVGLS reserve. We found a negative, non-
256 significant, association with maximal and resting HR and no association with baseline VO_2
257 uptake or CO.

258

259 The identified athletic LV remodeling corresponds to a dilation and increased myocardial
260 mass compared to the control LV, resulting in a more spherical LV. The ventricular dilation is
261 an adaptation to increase the stroke volume, and the increased sphericity and hypertrophy,
262 help to maintain wall stress limited when the pressure increases during exercise. The RV
263 presents a different type of remodeling: the global effect is an increase in volume, but that
264 increase is not homogeneous and is more prominent in the outflow. RV shape becomes
265 more elongated in the inlet, and there is a shift of volume from inlet to outflow, that is
266 dilated and more spherical. In conclusion, the RV remodeling corresponds more to a change
267 in shape rather than in size while the LV mostly dilates homogeneously.

268

269 The different behavior of the RV and LV can be explained from its intrinsic different
270 morphological characteristics, as well as the changes in loading conditions induced by
271 exercise. The RV is more compliant and elastic than the LV since LV cavity has not been
272 observed to increase acutely in size during extended submaximal exercise, while RV size can
273 increase up to 10% during moderate exercise (Claessen et al. 2014). Thus, the RV can change
274 shape acutely. The pulmonary artery and aorta also have very different behavior and
275 characteristics with the pulmonary artery being more compliant than the aorta (Slife et al.
276 1990; Marcus et al. 1994). Additionally, the pressure increases proportionally more in the
277 pulmonary artery during exercise, which translates to RV loading (Kovacs et al. 2009; La
278 Gerche et al. 2017). This is consistent with the observed remodeling in the RV outflow.
279 Another contributing factor, which could not be assessed using the currently available data,
280 might be the induced hypertrophy in the trabeculated RV apex, thus effectively reducing the
281 potential apical stroke volume and forcing the base to remodel accordingly.

282

283 Our data show that athletic remodeling at rest has a clear relationship with exercise
284 response: athletes with more remodeling can reach bigger VO_2 max and O_2 pulse. Via Fick's
285 Principle, O_2 uptake can be used to obtain an estimate of the CO during exercise, even when
286 the pulmonary extraction ratio (PER) is not known (Stringer et al. 1997). In (La Gerche et al.
287 2010), La Gerche et al. reported that the PER interindividual variability was independent of
288 physical training, so we can conclude that the differences in VO_2 max and O_2 pulse were due
289 to differences in CO and SV respectively. Since we found no correlation of athletic
290 remodeling and acute changes of ventricular geometry during exercise, we suggest that the
291 higher SV might be caused by increased deformation during exercise, explained by the weak
292 link between athletic remodeling and RV GLS reserve.

293 The long-term consequences of this remodeling are unknown, as follow-up is not available,
294 but remodeling seems positive, given that it is correlated with a better cardiovascular
295 response.

296

297 Limitations

298 The SA MRI images had lower quality in the apical part due to the low resolution in the axial
299 direction, and the presence of trabeculations making distinguishing between cavity and
300 myocardium difficult. Therefore, while standard practice, using only MRI SA to construct the
301 3D model is not ideal to evaluate the apical region and apical differences between the
302 populations might have stayed undetected due to this. Additionally, we did not manually
303 correct the automatic segmentations contours in the images, to better maintain the point-
304 to-point correspondence. We treated these segmentation errors as measurement error in
305 the analysis. Finally, the atria were not included in the image and therefore we could not
306 evaluate them using SSA.

307 The echocardiographic assessment was done pre- and post-exercise. Given the rapid
308 recovery of athletes, moving them quickly from the exercise bike to the scanning table can
309 affect the post-exercise analysis. Assessing shape during exercise would allow to better
310 understand the acute changes occurring during exercise and characterize the relationship
311 between athletic shape remodelling and cardiovascular response to exercise.

312 As stated, there is no follow-up data to confirm the positive effect of this remodeling. It must
313 be studied if this remodeling, that dilates the RV outflow, has any relationship with
314 arrhythmogenic right ventricle outflow in the long term.

315 Conclusion

316 This paper uses SSA to identify chronic resting shape remodeling induced by endurance sport
317 in both ventricles, using MRI. This remodeling consists of an LV increase in size and
318 myocardial mass, and a shape change in the RV: a shift of the volume distribution from the
319 inlet towards the outflow. Since RV remodeling is concentrated in the outflow, it adds more
320 evidence to the importance of the pulmonary circulation in athletes. After quantifying the
321 remodeling in all athletes, we found that during acute exercise, it is associated to maximal O_2
322 consumption, O_2 pulse and, weakly, to RV GLS reserve: athletes with more athletic
323 remodeling showed better cardiovascular exercise performance.

324

325 As future work, SSA could be used to find regional shape differences induced by pathological
326 remodeling (hypertrophic cardiomyopathies, arrhythmogenic right ventricle) that might have
327 an overlapping remodeling with the athlete's heart, and where current clinical
328 measurements are not well discriminating.

329

330 [Acknowledgements](#)

331 We thank Dr Weese and Dr Groth from Philips Research for the segmentation tool.

332 [Funding](#)

333 This study was partially supported by the Spanish Ministry of Economy and Competitiveness
334 (grant DEP2013-44923-P, TIN2014-52923-R; Maria de Maeztu Units of Excellence
335 Programme - MDM-2015-0502), el Fondo Europeo de Desarrollo Regional (FEDER) , the
336 European Union under the Horizon 2020 Programme for Research, Innovation (grant
337 agreement No. 642676 CardioFunXion) and Erasmus+ Programme (Framework Agreement
338 number: 2013-0040), "la Caixa" Foundation
339 (LCF/PR/GN14/10270005, LCF/PR/GN18/10310003), Instituto de Salud Carlos III
340 (PI14/00226, PI15/00130, PI17/00675) integrated in the "Plan Nacional I+D+I" and AGAUR
341 2017 SGR grant nº 1531.

342

343 [Conflicts of interest](#)

344 GB and MDC were working for Philips at the time of the work.

345 [Contributions](#)

346 ASM, MRL and FC acquired and measured the echocardiography and MRI controls data.
347 MSDG acquired and analyzed the echo data for the athletes. MSDG, FB and IB acquired and
348 analyzed the stress test. BDX, SPG and RJP acquired and analyzed the MRI data. The SSA was
349 done by GB, MAGB, CB and MDC. All authors participated in the data interpretation, reading
350 and approval the final manuscript.

351 [Ethical approval](#)

352 All procedures performed in studies involving human participants were in accordance with
353 the ethical standards of the institutional research committee (Comité ético de investigación
354 clínica del Hospital Clínic de Barcelona) and with the 1964 Helsinki declaration and its later
355 amendments or comparable ethical standards.

356

357 [References](#)

358 Ainsworth BE, Haskell WL, Herrmann SD, et al (2011) 2011 compendium of physical
359 activities: A second update of codes and MET values. Med. Sci. Sports Exerc.

360 Albert RK, Spiro SG, Jett JR (2008) Clinical respiratory medicine

- 361 Claessen G, Claus P, Ghysels S, et al (2014) Right ventricular fatigue developing during
362 endurance exercise: An exercise cardiac magnetic resonance study. *Med Sci Sports*
363 *Exerc.* <https://doi.org/10.1249/MSS.0000000000000282>
- 364 Cootes TF, Taylor CJ, Cooper DH, Graham J (1995) Active Shape Models-Their Training and
365 Application. *Comput Vis Image Underst* 61:38–59.
366 <https://doi.org/10.1006/cviu.1995.1004>
- 367 D’Andrea A, La Gerche A, Golia E, et al (2015) Right heart structural and functional
368 remodeling in athletes. *Echocardiography* 32:11–22.
369 <https://doi.org/10.1111/echo.12226>
- 370 De Craene M, Duchateau N, Tobon-Gomez C, et al (2012) SPM to the heart: Mapping of 4D
371 continuous velocities for motion abnormality quantification. In: *Proceedings -*
372 *International Symposium on Biomedical Imaging*
- 373 DeLong ER, DeLong DM, Clarke-Pearson DL (1988) Comparing the Areas under Two or More
374 Correlated Receiver Operating Characteristic Curves: A Nonparametric Approach.
375 *Biometrics.* <https://doi.org/10.2307/2531595>
- 376 Dryden L, Mardia K V. (1998) *Statistical Shape Analysis.* In: John Wiley & Son. p 347
- 377 Du Bois D, Du Bois EF (1916) A formula to estimate the approximate surface area if height
378 and weight be known. *Arch Intern Med* XVII:863–871.
379 <https://doi.org/10.1001/archinte.1916.00080130010002>
- 380 Ecabert O, Peters J, Weese J, et al (2006) Automatic heart segmentation in CT: Current and
381 future applications. *Medicamundi* 50:12–17
- 382 Kovacs G, Berghold A, Scheidl S, Olschewski H (2009) Pulmonary arterial pressure during rest
383 and exercise in healthy subjects: A systematic review. *Eur. Respir. J.*
- 384 La Gerche A, Baggish AL, Knuuti J, et al (2013) Cardiac imaging and stress testing
385 asymptomatic athletes to identify those at risk of sudden cardiac death. *JACC*
386 *Cardiovasc Imaging* 6:993–1007. <https://doi.org/10.1016/j.jcmg.2013.06.003>
- 387 La Gerche A, Burns AT, Mooney DJ, et al (2012) Exercise-induced right ventricular
388 dysfunction and structural remodelling in endurance athletes. *Eur Heart J* 33:998–1006.
389 <https://doi.org/10.1093/eurheartj/ehr397>
- 390 La Gerche A, Maclsaac AI, Burns AT, et al (2010) Pulmonary transit of agitated contrast is
391 associated with enhanced pulmonary vascular reserve and right ventricular function
392 during exercise. *J Appl Physiol.* <https://doi.org/10.1152/jappphysiol.00457.2010>
- 393 La Gerche A, Rakhit DJ, Claessen G (2017) Exercise and the right ventricle: A potential
394 Achilles’ heel. *Cardiovasc. Res.*
- 395 Lang RM, Badano LP, Mor-Avi V, et al (2015) Recommendations for cardiac chamber
396 quantification by echocardiography in adults: An update from the American society of
397 echocardiography and the European association of cardiovascular imaging. *Eur Heart J*
398 *Cardiovasc Imaging.* <https://doi.org/10.1093/ehjci/jev014>
- 399 Marcus RH, Korcarz C, McCray G, et al (1994) Noninvasive method for determination of
400 arterial compliance using Doppler echocardiography and subclavian pulse tracings:

401 Validation and clinical application of a physiological model of the circulation.
402 Circulation. <https://doi.org/10.1161/01.CIR.89.6.2688>

403 Peters J, Ecabert O, Meyer C, et al (2010) Optimizing boundary detection via Simulated
404 Search with applications to multi-modal heart segmentation. *Med Image Anal.*
405 <https://doi.org/10.1016/j.media.2009.10.004>

406 Rhodes J, Garofano RP, Bowman FO, et al (1990) Effect of right ventricular anatomy on the
407 cardiopulmonary response to exercise. Implications for the Fontan procedure.
408 *Circulation* 81:1811–7

409 Robin X, Turck N, Hainard A, et al (2011) pROC: An open-source package for R and S+ to
410 analyze and compare ROC curves. *BMC Bioinformatics.* [https://doi.org/10.1186/1471-](https://doi.org/10.1186/1471-2105-12-77)
411 [2105-12-77](https://doi.org/10.1186/1471-2105-12-77)

412 Ross RM, Beck KC, Casaburi R, et al (2003) ATS/ACCP Statement on Cardiopulmonary
413 Exercise Testing (multiple letters). *Am J Respir Crit Care Med* 167:1451.
414 <https://doi.org/10.1164/ajrccm.167.10.950>

415 Sanz-de la Garza M, Giraldeau G, Marin J, et al (2017) Influence of gender on right ventricle
416 adaptation to endurance exercise: an ultrasound two-dimensional speckle-tracking
417 stress study. *Eur J Appl Physiol* 117:389–396. [https://doi.org/10.1007/s00421-017-](https://doi.org/10.1007/s00421-017-3546-8)
418 [3546-8](https://doi.org/10.1007/s00421-017-3546-8)

419 Schmied C, Borjesson M (2014) Sudden cardiac death in athletes. *J Intern Med* 275:93–103.
420 <https://doi.org/10.1111/joim.12184>

421 Sitges M, Merino B, Butakoff C, et al (2017) Characterizing the spectrum of right ventricular
422 remodelling in response to chronic training. *Int J Cardiovasc Imaging* 33:331–339.
423 <https://doi.org/10.1007/s10554-016-1014-x>

424 Slife DM, Latham RD, Sipkema P, Westerhof N (1990) Pulmonary arterial compliance at rest
425 and exercise in normal humans. *Am J Physiol - Hear Circ Physiol*

426 Stringer WW, Hansen JE, Wasserman K (1997) Cardiac output estimated noninvasively from
427 oxygen uptake during exercise. *J Appl Physiol* 82:908–12

428 Varano V, Piras P, Gabriele S, et al (2018) The decomposition of deformation: New metrics to
429 enhance shape analysis in medical imaging. *Med Image Anal* 46:35–56.
430 <https://doi.org/10.1016/j.media.2018.02.005>

431 Varela M, Bisbal F, Zacur E, et al (2017) Novel computational analysis of left atrial anatomy
432 improves prediction of atrial fibrillation recurrence after ablation. *Front Physiol* 8:68.
433 <https://doi.org/10.3389/FPHYS.2017.00068>

434 Zhang X, Cowan BR, Bluemke DA, et al (2014) Atlas-based quantification of cardiac
435 remodeling due to myocardial infarction. *PLoS One.*
436 <https://doi.org/10.1371/journal.pone.0110243>

437

438 Tables

439 *Table 1 Demographics and echocardiographic functional measurements of the population, in the format of mean (STD).*

	Athletes	Controls	p-value
Age [y]	35.4(6.1)	33.4(3.8)	0.013
BSA [m ²]	1.78(0.19)	1.86(0.20)	0.005
Weight [kg]	66.8(11.3)	73.5(15.1)	0.001
Height [m]	1.71(0.09)	1.73(0.08)	0.151
Women [%]	42(48%)	32(44%)	0.938
HR - echo [bpm]	57.2(8.4)	65.8(10.6)	< 0.001
LV EF [%]	54.6(4.4)	62.6(5.6)	< 0.001
SV [ml/m ²]	47.5(9.5)	40.2(8.6)	< 0.001
CO [l/min/m ²]	2.7(0.6)	2.6(0.5)	0.302
RV FAC [%]	45.2(5.2)	45.6(8.7)	0.767
TAPSE [mm]	25.9(2.9)	25.3(3.4)	0.197
VO ₂ peak [l/min/m ²]	1.63(0.28)	1.11(0.28)	< 0.001

440

441 (BSA: body surface area, HR: heart rate, LV EF: left ventricular ejection fraction, SV: stroke
 442 volume, CO: Cardiac output, RV FAC: right ventricular fractional area change, TAPSE:
 443 tricuspid annular plane systolic excursion, VO₂ max: Maximal oxygen uptake)

444

445 *Table 2 Comparison of the MRI- based measurements between athletes and controls. All measurements were computed*
 446 *from the MRI-derived 3D model .*

	Athletes	Controls	p-value
LV EDV [mL/m ²]	101.7(17.4)	82.9(12.1)	< 0.001
LV Mass (3D) [g/m ²]	83.7(14.0)	71.7(11.4)	< 0.001
LV LA[mm/ m ²]	53.9(4.2)	49.4(4.2)	< 0.001
LV OT [mm/ m ²]	14.6(1.0)	13.4(0.9)	< 0.001
RV EDV [mL/m ²]	108.3(22.6)	86.4(15.7)	< 0.001
RV EDA [cm ² /m ²]	18.0(2.6)	15.7(2.2)	< 0.001
RV LA [mm/m ²]	51.8(3.8)	47.2(3.9)	< 0.001
RV Basal Dimension [mm/m ²]	28.1(2.5)	25.8(2.4)	< 0.001
RV OT [mm/m ²]	16.6(1.4)	15.0(1.1)	< 0.001

447

448 (LV EDV: left ventricular end-diastolic volume, LV LA: left ventricular long axis, LV OT: left
 449 ventricular outflow tract, RV EDV: right ventricular end-diastolic volume, RV EDA: right
 450 ventricular end-diastolic area RV LA: right ventricular long axis, RV OT: right ventricular
 451 outflow tract)

452

453 *Table 3 : Results of the MVR to check the relationship between shape remodeling score to different functional parameters*
454 *during exercise. Only athletes are included in this analysis. The p-values were obtained by comparing the regression model*
455 *involving the athletic remodeling score and the confounders with a model that uses only confounders with a Fisher F-test.*

	Standardized coefficient	R²	P Value
Resting HR	-0.18	0.08	0.03
Maximal HR	-0.17	0.19	0.08
Baseline VO ₂	-0.10	0.09	0.50
Peak VO ₂	0.20	0.49	<0.01
Peak oxygen pulse	0.26	0.51	< 0.001
Baseline RV GLS	-0.17	0.29	0.11
Post-exercise RV GLS	0.04	0.41	0.69
RVGLS resere	0.29	0.24	0.03
Resting LV GLS	0.02	0.31	0.84
Post-exercise LV GLS	0.11	0.30	0.23
Resting LV EDV	0.67	0.73	< 0.001
LV myocardial volume	0.50	0.72	< 0.001
LV EDV increase ratio	0.02	0.01	0.70
Resting RV EDV	0.61	0.69	< 0.001
RV EDA increase ratio	-0.10	0.05	0.24

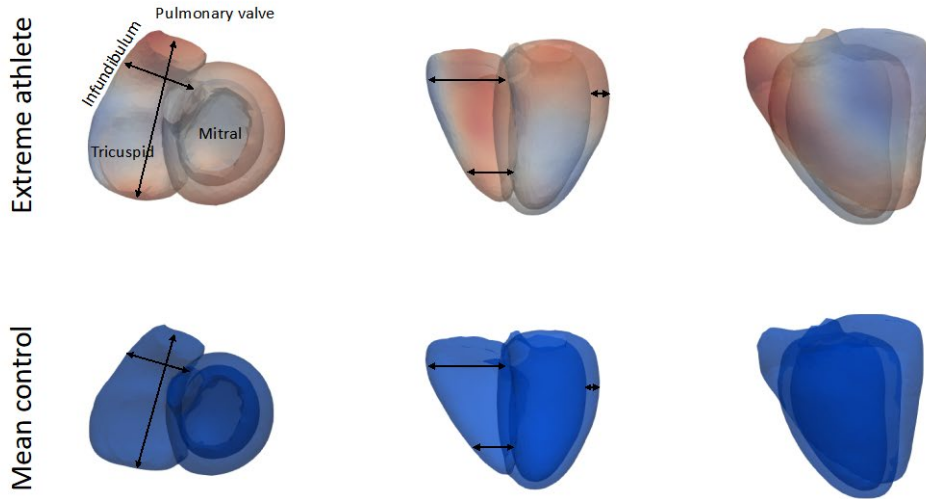
456

457 (VO₂: oxygen uptake, RV GLS: right ventricular global longitudinal strain, LV GLS: left
458 ventricular global longitudinal strain, LV EDV: left ventricular end-diastolic volume, RV
459 EDV: right ventricle end-diastolic volume)

460

461
462

Figures



463
464

465 *Figure 1 Most discriminant shape mode that distinguishes the RV from athletes and controls. The upper row corresponds to*
466 *a representative extreme athlete (population mean + 3STD of athletic remodeling), and the lower one to the mean shape of*
467 *the non-athletes. The three views correspond to: a view of the base from the atria (left), a longitudinal view of the inferior*
468 *RV and LV walls (center), and a longitudinal view of the LV free wall (center). The red-blue color map indicates in red the*
469 *regions that present more remodeling, and the purple lines the observed differences. Both ventricles are very different from*
470 *the controls, but while the LV mostly scale, more regional shape changes occur in the RV, especially in the outflow.*

471
472